Defense Technical Information Center Compilation Part Notice

ADP011765

TITLE: Low-Dispersive Coplanar Waveguides and Thin-Film Microstrip Lines for Sub-mm Wave Monolithic Integration

DISTRIBUTION: Approved for public release, distribution unlimited

This paper is part of the following report:

TITLE: International Conference on Terahertz Electronics [8th], Held in Darmstadt, Germany on 28-29 September 2000

To order the complete compilation report, use: ADA398789

The following component part numbers comprise the compilation report:
ADP011730 thru ADP011799

Low-dispersive Coplanar Waveguides and Thin-film Microstrip Lines for Sub-mm Wave Monolithic Integration

Frank Schnieder and Wolfgang Heinrich

Abstract **– Planar sub-millimeterwave transmission-line structures suitable for monolithic integration are discussed. The results show that both miniaturized coplanar waveguides and appropriate thin-film microstrip configurations provide low-dispersive propagation properties up to 1 THz. The paper discusses radiation and dispersion effects as well as basic rules how CPWs should be designed in order to reach the desired sub-mm wave performance.**

I. Introduction

Monolithic integration of sub-mm wave components is still an ambitious goal. Today, most of these systems are realized as a hybrid circuit. But any interconnect causes reflections, and already small parasitics may become critical at Terahertz frequencies. Accordingly, one tries to integrate as many elements as possible together with the semiconductor device, also in the hybrid case. For this purpose, transmission-line structures are required that offer low dispersion together with reasonably low loss. At the same time, they must be compatible with the common planar circuit geometry and processing scheme.

Particular candidates are the coplanar waveguide (CPW) and the thin-film microstrip line (TFMSL), which is realized on top of the substrate using polyimide or BCB (bis-benzocyclobutene) as dielectric layer of 1..20 µm thickness. This allows to scale down strip width and thus the total line dimensions. Our investigations show that such thin-film microstrip lines can be used up to 1 THz with excellently low dispersion. Coplanar waveguides with scaled-down dimensions achieve similar properties. Additional to the common CPW design criteria, however, one has to take into account higher-order modes and radiation loss.

II. Thin-film Microstrip Line (TFMSL)

In contrast to the conventional microstrip, the TFMSL is realized on top of the substrate using a thin polyimide or BCB dielectric layer. Fig. 1 shows the cross section. The fields are concentrated in the dielectric layer and the ground metalization provides shielding against the substrate. Therefore, one may use lossy material as a substrate, e.g., low-resistivity silicon. The typical BCB or polyimide thicknesses are in the range 1...25 µm. This is considerably smaller than for the conventional microstrip case. As a consequence, the line dimensions, i.e., strip width, can be scaled down, which increases the frequency range of quasi-TEM operation well into the Terahertz region. One has to pay for this, of course, by larger attenuation due to conductor loss.

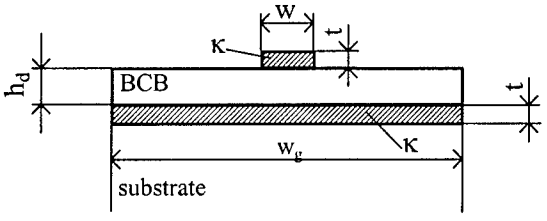

Fig. 1: TFMSL cross-section metal (κ denotes metal conductivity, the thickness is t = 0.8 µm, and ground width w_g >> w, 5 Ωcm Si is used as a substrate and BCB as dielectric).

Fig. 2 presents simulated and measured results for such a TFMSL with 2.7 µm thick BCB dielectric. The 7.4 µm wide strip yields 50 Ω characteristic impedance. For simulation, the full-wave mode-matching method of [1] is applied that rigorously accounts for metal loss. The experimental data refers to electro-optic measurements at the RWTH Aachen [2].

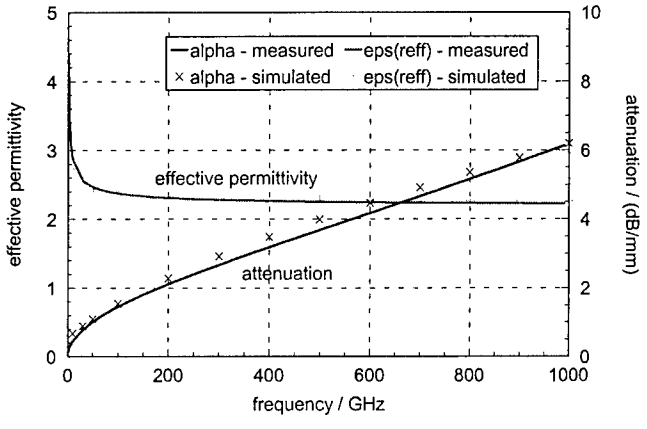

Fig. 2: Effective permittivity ε_{reff} and attenuation α as a function of frequency (50 Ω TFMSL according to Fig. 1 with strip width w = 7.4 µm, BCB layer with thickness h_d = 2.7 µm, $\tan\delta_\varepsilon$ = 0.015, and metal conductivity κ = 30 S/µm; Si substrate with ρ = 5 Ωcm; simulation data [1] and electro-optic measurements [2]).

Effective permittivity $\varepsilon_{reff} = (\beta/\beta_0)^2$ and attenuation α are plotted against frequency up to 1 THz. Effective permit-

Frank Schnieder and W. Heinrich are with the Ferdinand-Braun-Institut für Höchstfrequenztechnik (FBH), Albert-Einstein-Strasse 11, D-12489 Berlin / Germany. This work is supported by the Deutsche Forschungsgemeinschaft (DFG) under contract No. He 1676/10.

tivity exhibits a negative slope at the lower frequency end, which is caused by metal loss, and then approaches a constant value. This demonstrates the quasi-TEM properties and the excellently low dispersion. The reasons are the small BCB thickness and strip width together with the low permittivity of the BCB ($\varepsilon_r = 2.7$). On the other hand, the miniaturized conductor dimensions lead to attenuation values of about 5 dB/mm at 1 THz. However, for short connecting lines within a circuit, this is acceptable. Moreover, one can trade lower loss for higher dispersion by increasing the line dimensions.

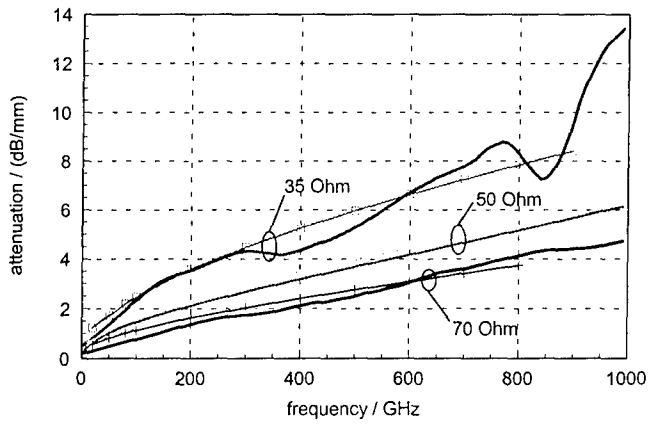

Fig. 3: Attenuation as a function of frequency for a 35 Ω, 50 Ω, and a 70 Ω line (all data as in Fig. 2, except for w = 8 μm, h_d = 1.7 μm for the 35 Ω case, and w = 8 μm, h_d = 5.4 μm for the 70 Ω line).

The characteristic impedance can be adjusted by choosing a suitable w/h_d ratio. Fig. 3 illustrates the attenuation curves for the 50 Ω TFMSL of Fig. 2 together with a 35 Ω and a 70 Ω geometry. Larger impedance values can be achieved by increasing h_d or decreasing w. One should note that, despite of the low-ε_r dielectric, the full impedance range down to 30 Ω can be realized within the common technological limitations.

III. Coplanar Waveguide (CPW)

The CPW type most appropriate for sub-mm-wave applications is that with finite ground width and substrate thickness. Fig. 4 illustrates the cross-section. Only modes with even symmetry are considered (for analysis, a magnetic symmetry wall is placed in the center). As for the TFMSL, high-resistivity Si is used as a substrate. The substrate resistivity plays an important role in the CPW case, because, in contrast to the TFMSL, the fields penetrate deeply into the substrate and thus attenuation is strongly affected by substrate material loss. In order to keep dispersion and non-TEM effects low the ground-to-ground spacing w+2s has to be scaled down with increasing frequency of operation.

Fig. 5 presents simulation results and electro-optic measurements [2] for such a miniaturized CPW in the frequency range up to 1 THz. The simulation data refers to a mode-matching approach [1], which considers conductor loss but neglects radiation, and FDTD calculations [6], which include radiation but assume lossless conductors. Thus, the realistic attenuation value is the sum of both contributions, which closely fits the measured data. Two different ground-plane widths w_g of 160 μm and 16 μm are studied in Fig. 5.

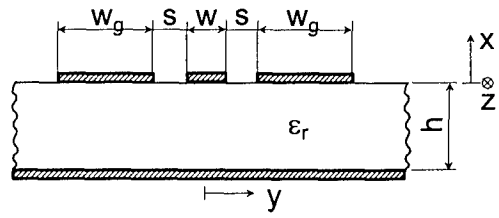

Fig. 4: The CPW geometry considered (substrate: high-resistivity Si with $\varepsilon_r = 11.67$).

Generally, dispersion in ε_{reff} is small, but larger than for the TFMSL structures treated before. This can be attributed to the larger lateral line dimensions of the CPW (note that the CPW ground-to-ground spacing w+2s in Fig. 5 is 40 μm compared to 8 μm strip width for the TFMSL in Figs. 2 and 3).

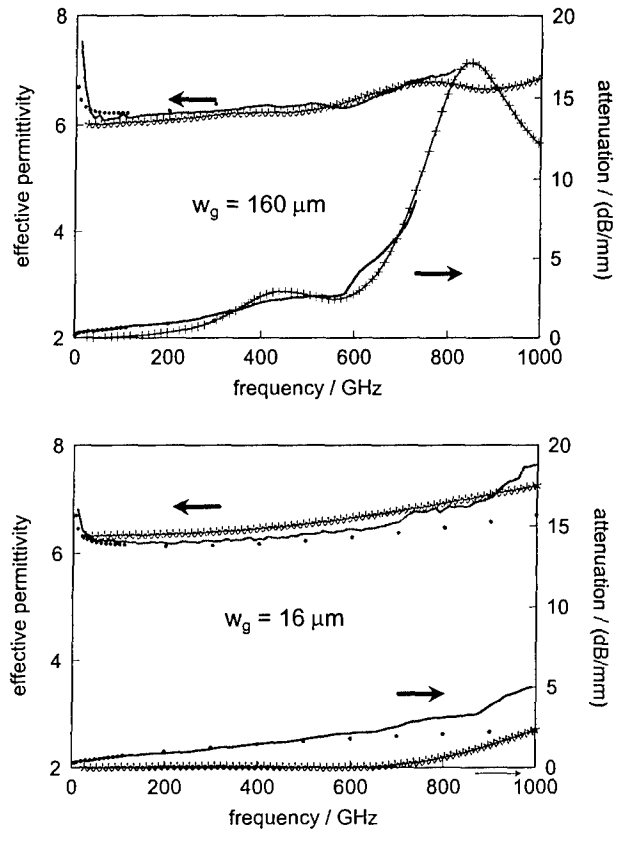

Fig. 5: CPW effective permittivity and attenuation as a function of frequency for two different ground-plane widths w_g (solid lines: electro-optic measurements [2], symbols: mode-matching analysis [1] for closed structure, curves with symbols: FDTD simulation [6]; for geometry and parameter see Fig. 4 with w = 16 μm, s = 12 μm; metal conductivity 35 S/μm, 380 μm thick Si substrate).

Studying the ε_{reff} characteristics in Fig. 5 in more detail, a slight peak near 700 GHz is observed for the larger ground value. This will be explained in the context of Fig. 7. In the low GHz range, one has the typical increase

in ε_{reff} caused by conductor loss as observed for the TFMSL. More important, however, are the attenuation results. They show clearly that the reduced ground width leads to a considerably lower attenuation level.

In this context, it is interesting to study the differences between the two cases for finite and infinite ground width. In Fig. 6, simulation data [7] for $w_g = 80$ µm (both infinite substrate thickness h and h = 200 µm) are plotted together with the well-known approximation of [3], which assumes infinite ground width and substrate. For the latter one, attenuation follows an f^3 rule, whereas finite w_g leads to an f^5 dependence. This finding supports the statement that w_g is indeed an important parameter regarding CPW radiation loss. Substrate thickness h, on the other hand, determines the onset of radiation, but does not exert a strong quantitative influence.

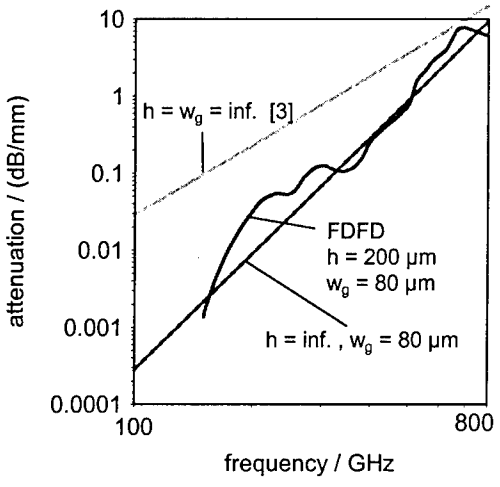

Fig. 6: CPW attenuation due to radiation against frequency (FDFD analysis [7] of the geometry in Fig. 4 with ideally conducting metalizations, w = 16 µm, s = 12 µm, w_g = 80 µm, and h = 200 µm as compared to analytical formulas with h = for w_g = [3][5] and w_g = 80 µm [7], respectively).

IV. CPW Design Rules

In the CPW case, one has not only to account for dispersion and radiation of the CPW mode but also to consider higher-order modes, which may adversely affect propagation characteristics or cause parasitic effects in the packaged circuit (see, e.g., [4]). These higher-order modes are related to substrate thickness h and ground width w_g (see [7]). Fig. 7 presents the effective permittivity values for the 2 fundamental modes (CPW and PPL) and the first 3 higher-order ones (HM). The CPW structure of Fig. 5 is studied with a realistic w_g value of 80 µm and a 200 µm thick conductor-backed substrate.

First, one should note that the finite extent of the ground plane ($w_g <$) shifts onset of radiation into lateral surface-wave modes to higher frequencies (one has f = 0 for $w_g =$), but it does not prevent existence of a parallel-plate like (PPL) mode (sometimes referred to as the microstrip-like mode). This PPL mode is present in any case as long as conductor-backed substrates are used. In practical circuits, they form a parasitic bypass between discontinuities and interconnects, which reduces isolation and may cause instabilities in high-gain systems.

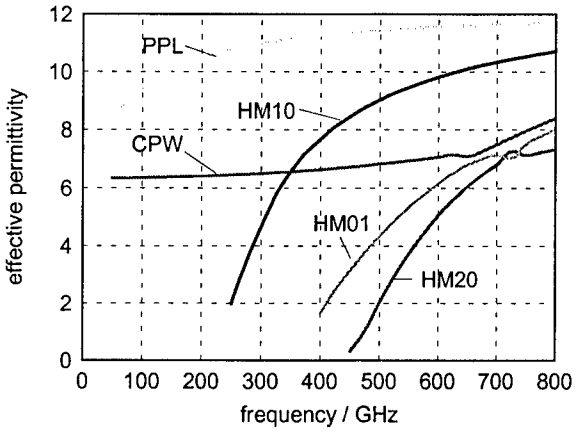

Fig. 7: Effective permittivity of fundamental modes (CPW, PPL) and higher-order modes (HM) against frequency (FDFD analysis of the geometry in Fig. 4 with ideally conducting metalizations, w = 16 µm, s = 12 µm, w_g = 80 µm, and h = 200 µm).

The PPL mode exhibits a microstrip-like dispersion behavior with a strong increase in ε_{reff} with growing frequency, whereas the CPW mode phase constant remains almost constant up to about 600 GHz in our case. Here, critical effects are not the non-TEM dispersion itself, but interaction with higher-order modes.

For the geometry studied in Fig. 7, the first higher-order mode (HM10) as well as HM20 are related to substrate thickness h, i.e., they can be shifted towards higher frequencies by reducing h. The second higher order mode, HM01, is due to the lateral line width, i.e., primarily ground-plane width w_g. Thus, one concludes that for reliable high-frequency operation, both h and w_g have to be chosen small enough to prevent the occurrence of higher-order modes. Introducing an approximate model one derives a simple formula providing the corresponding design values as a function of the maximum frequency f_{max} (see [7]):

$$\mathrm{Max}\left\{h, \frac{w}{2} + s + w_g\right\} \leq \frac{1}{f_{max} \cdot \sqrt{2\mu_0\varepsilon_0(\varepsilon_r - 1)}} \quad (1)$$

Using (1) one can easily adjust substrate thickness h and ground-width w_g to the desired frequency range. Note that a further reduction of w_g can be of advantage, because it reduces attenuation (see Section III).

V. CPW versus TFMSL

As described in the preceding sections, CPW and TFMSL both are suitable sub-mm-wave transmission lines. So far, however, a direct comparison is missing. This is presented in Fig. 8. In order to obtain useful information from such a comparison, two structures are compared that provide the same characteristic impedance and are comparable in size. The latter condition involves some uncer-

tainties as to lateral line size. In the CPW case (see Fig. 4), the total line width ($w+2s+2w_g$) represents a good measure, also regarding the lateral spacing from neighboring lines required to prevent crosstalk. For the TFMSL, it is more difficult to define such a figure since the strip width w (see Fig. 1) is much smaller than the spacing needed because of crosstalk. A value of 5 times the dielectric thickness h_d gives good isolation so that the total width allocated by a TFMSL is approximately $10h_d+w$. Following these considerations, in Fig. 8 both for CPW line width ($w+2s+2w_g$) and TFMSL width ($10h_d+w$) the same value of 62 μm is chosen.

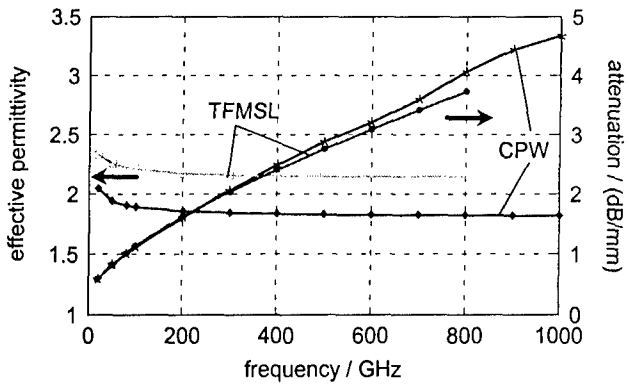

Fig. 8: Comparison of CPW and TFMSL (70 Ω lines of equivalent size): effective permittivity and attenuation against frequency (simulation data [1]); TFMSL dimensions as in Fig. 1 with $w = 8$ μm, $h_d = 5.4$ μm, CPW with $w = 13$ μm, $s = 3.5$ μm, $w_g = 21$ μm on 25 μm thick BCB over 5 Ωcm Si substrate (see Fig. 4 with layered substrate); Al metalization with $\kappa = 23.5$ S/μm, BCB: $\varepsilon_r = 2.7$, $\tan\delta_\varepsilon = 0.015$.

The results demonstrate that both line types show comparable attenuation. The same statement holds for dispersion characteristics, which is negligible up to at least 800 GHz. Naturally, effective permittivity for the CPW is lower than for the TFMSL, because in the latter case the field portion within the dielectric is larger. Briefly speaking, the differences with respect to dispersion and attenuation are minor and do not justify a clear preference for one of the line types.

There is one major difference, however, which is important for circuit design: The BCB dielectric with its low permittivity value is very beneficial in reducing dispersion. But, at the same time, it lowers characteristic impedance for a given conductor geometry. So, given a fixed impedance value, e.g., 50 Ω, one has to compensate for this by adjusting conductor dimensions accordingly. For the TFMSL, this is obtained easily (see Figs. 2 and 3). For the CPW, however, this requires a very small slot-to-strip width ratio s/w. This can be seen from the data in Fig. 8, where for a 70 Ω CPW a slot width of only 3.5 μm is necessary. For a 50 Ω CPW, situation is worse: assuming 40 μm ground-to-ground spacing (as treated in Sec. III) on a dielectric with $\varepsilon_r = 3$ yields a center strip width w of 35 μm and a slot width $s = 2.5$ μm, which is beyond the technological limitations of the common processes.

VI. Conclusions

- Both TFMSL and miniaturized CPW are suitable for sub-mm-wave monolithic applications. Scaling down the dimensions yields excellent dispersion properties and low radiation, of course, at the expense of higher conductor loss. Attenuation levels are in the range of 5..10 dB/mm at 1 THz. Given the short line lengths in monolithic structures this is acceptable.

- While TFMSL and CPW achieve comparable performance in terms of dispersion and loss, there are differences in flexibility. The TFMSL properties do not depend on substrate quality and it covers a wider impedance range. The CPW impedance range, on the other hand, is restricted more severely by technological limitations, particularly the minimum slot width. This causes problems when realizing CPWs on low-permittivity dielectrics. Then the 50 Ω value may be below the available impedance range.

VII. Acknowledgements

Part of this work was pursued in a collaboration with the RWTH Aachen, Lehrstuhl für Halbleitertechnik II (Prof. H. Kurz), where the TFMSL and CPW structures were fabricated and the electro-optic measurements were performed. The authors gratefully acknowledge this and would like to thank particularly H. Roskos, H.-M. Heiliger, and T. Pfeiffer for their contributions.

VIII. References

1. W. Heinrich, "Full-wave analysis of conductor losses on MMIC transmission lines", IEEE Transactions MTT, vol. 38, 1990, pp. 1468-1472.
2. H.-M. Heiliger, M. Nagel, M. Setz, H. G. Roskos, H. Kurz, F. Schnieder, W. Heinrich, "Thin-film microstrip lines for mm and sub-mm-wave on-chip interconnects". 1997 IEEE MTT-S Int. Microwave Symp. Digest, vol. 2, pp. 421-424.
3. M.Y. Frankel, S. Gupta, J.A. Valdmanis, and G.A. Mourou, "Terahertz attenuation and dispersion characteristics of coplanar transmission lines," IEEE Trans. Microwave Theory Tech. vol. 39, pp. 910-915, June 1991.
4. H. Shigesawa, M. Tsuji, and A.A. Oliner, "Conductor-backed slot line and coplanar waveguide: dangers and full-wave analyses," 1988 Int. Microwave Symp. Digest, Vol. I, pp. 199-202.
5. D.B. Rutledge, D.P. Neikirk, and D.P. Kasilingam, in "Infrared and Millimeter Waves", vol. 10, "Millimeter Components and Techniques", chapt. 1: Integrated-circuit antennas", Editor: K.J. Button, New York, Academic Press, 1983.
6. N.-H. Huynh and W. Heinrich, "FDTD analysis of sub-millimeter wave CPW with finite-width ground metalization," IEEE Microwave and Guided Wave Letters, Vol. 7, No. 12, pp. 414-416, Dec. 1997.
7. W. Heinrich, F. Schnieder, and T. Tischler, "Dispersion and radiation characteristics of conductor-backed CPW with finite ground width," 2000 Int. Microwave Symp. Digest, vol. 3, pp. 1663-1666.